

Synthesis of Parametric Map from Raw Ultrasound B-Scan Data

R. Jurkonis, S. Daukantas, A. Janušauskas, A. Lukoševičius

Biomedical Engineering Institute, Kaunas University of Technology,

Studentu str. 65, LT-51369, Kaunas, Lithuania, phone: +370 37 407119, e-mail: rytis.jurkonis@ktu.lt

V. Marozas, D. Jegelevičius

Department of Signal Processing, Kaunas University of Technology,

Studentu str. 50, LT-51368, Kaunas, Lithuania, phone: +370 37 351206, vaidotas.marozas@ktu.lt

Introduction

Ultrasound echoscopy of eye is routine investigation in ophthalmology practice; it is available at university hospitals and at private specialists' clinics as well. Biometrical evaluation of eye is possible by intraocular images obtained non-invasively [1, 2]. The objective data is valuable for diagnostics and treatment monitoring [3]. However, in case of complicated oncological diseases e.g. in planning and monitoring of brachytherapy [4], the ophthalmologists are lacking suitable informative parameters for differential diagnostics [3, 5] as well as prognostic methodologies to be implemented in clinical practice [4, 5]. Review of ultrasound diagnostic research in the field of ophthalmological oncology shows the possibilities of tumor tissue characterization using radio-frequency (RF) signal processing since modern analysis of RF ultrasound signal could give valuable parameters for tumor characterization. The preliminary trials with animal models had shown a feasibility of this approach [6]. Therefore the development of the expert system based on ultrasonic radiofrequency signals had been chosen [7].

The aim of this paper is to develop the mapping methodology by the use of amplitude and frequency parameters of raw ultrasound B-scan signal. The first task in this direction was the implementation of software-based processing and visualization of RF ultrasound signals acquired from the conventional B-scan imaging system.

Signal capturing methodology

The ultrasound pulses were sent and echography signals received by proprietary B scan ultrasonic imaging system Mentor Advent™ A/B (Mentor Ophthalmics, Norwell, MA, USA). Broadband (11 MHz) ultrasonic transducer of the system was mechanically scanned within the 50° sector. The analog ultrasonic radio frequency signals (raw data) were acquired directly after primary amplifiers, digitized using PC oscilloscope PicoScope 5203 (Pico Technology Ltd., Cambridgeshire, UK) with sampling frequency 250 MHz and amplitude resolution 8 bits and sent to PC. The hardware structure is presented in

Fig. 1. Programmable synchronizer was developed for the flexible control over the system and for the effective use of the large memory buffer (up to 32 MB) of the PC oscilloscope which enabled to capture online whole B-scan ultrasound RF frame from the standard phantom.

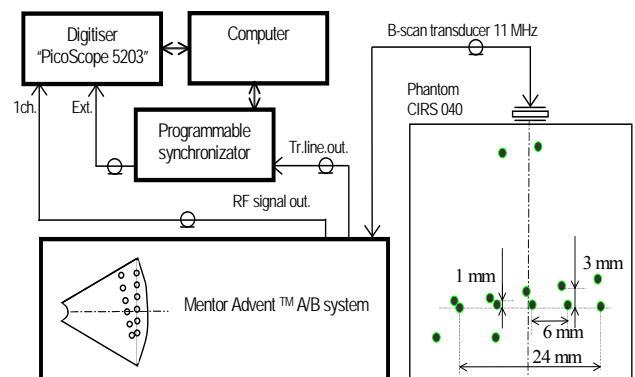


Fig. 1. Experimental setup for evaluation of mapping methodology

General purpose multi-tissue ultrasound phantom, Model 040 (CIRS Inc., Norfolk, Virginia, USA) [10] was used during experiments. This phantom has target group (group of point reflectors) for evaluation of imaging resolution. The targets in the phantom were nylon monofilament wires of 0,1 mm diameter immersed in the background material (Zerdine) for the mimicking liver tissue microstructure, which is characterized by $0,5 \pm 0,05 \text{ dB/MHz cm}@5\text{MHz}$ attenuation coefficient and $1540 \pm 10 \text{ m/s}$ speed of ultrasound. The targets in groups of are spaced by 0,5; 1, 2, 3 and 4 mm intervals ($\pm 0,2 \text{ mm}$), at the depth of 25 mm, the distances among groups of targets are $6 \pm 0,2 \text{ mm}$.

Processing and mapping of RF signal parameters

The threshold detector was used to rearrange the acquired samples of raw ultrasound signal into a matrix containing 250 rows (one frame of B - scan). The rows from the matrix were processed using digital signal processing algorithms in order to extract signal parameters

and then to convert into the B-scan sector image of the parametric map.

For the visualization and mapping we applied three signal processing algorithms: signal demodulation for echo amplitude mapping; short time Fourier transform (STFT) based algorithms for mapping of mean instantaneous frequency (MIF) and mean instantaneous bandwidth (MIB) of raw echosignal spectrum. RF signal magnitude (or instantaneous magnitude (IM)) is widely used for rendering of B type ultrasound scans. IM represents variation of RF signal envelope in time. The best way to calculate IM parameter digitally is to find the magnitude of an analytical signal:

$$x_{IM}(t) = \sqrt{x^2(t) + x_H^2(t)}. \quad (1)$$

where $x(t)$ is the real part and $x_H(t)$ – the imaginary part of analytical signal $x_A=x(t)+jx_H(t)$. Real part is the acquired signal while imaginary part is calculated using the Hilbert transform [8]:

$$x_H(t) = \frac{1}{\pi} \int_{-\infty}^{\infty} \frac{x(\tau)}{t - \tau} d\tau. \quad (2)$$

Logarithmic values of IM were used for the modulation of B-scan image color and obtaining the sector image.

The MIF parameter of ultrasound RF signal was calculated according to the equation [8]:

$$f_{MIF}(t) = \int_{-\infty}^{+\infty} f \cdot STFT(t, f) df / \int_{-\infty}^{+\infty} STFT(t, f) df, \quad (3)$$

where $STFT(t, f)$ is a short time Fourier transform of each ultrasound RF signal (raw of the matrix of captured RF B-scan). STFT's were evaluated using these empirically optimized parameters: the shape of the window - Gaussian, the length of time window - 2,5 μ s (it is equivalent to 3,87 mm in a distance scale), overlap factor of windows – 98 %.

The MIB parameter of ultrasound RF signal was evaluated according to following equation [8]:

$$f_{MIB}(t) = \sqrt{\int_{-\infty}^{+\infty} (f - f_{MIF}(t))^2 \cdot STFT(t, f) df} / \int_{-\infty}^{+\infty} STFT(t, f) df. \quad (4)$$

RF signal parameters were used for the synthesis of the parametric map. The B-scan sector image was synthesized on the PC screen using time sequences of ultrasound signal parameters (IM, MIF and MIB) of each scan line using following scan conversion equations [9]:

$$\begin{cases} x(t) = x_0 + 0,5 \cdot c \cdot t \cdot \cos(\gamma) \\ y(t) = y_0 + 0,5 \cdot c \cdot t \cdot \sin(\gamma) \end{cases}. \quad (5)$$

Here $x(t)$ and $y(t)$ – projections of the vector following the ultrasound beam, x_0 and y_0 – initial coordinates, c – mean ultrasound velocity in the eye tissues (assumed 1550 m/s), t – time, γ – the instantaneous angle of the ultrasound beam (assumed range of $\gamma=\pm 25^\circ$).

Evaluation of mapping results

In this section we present results of processing and

mapping using MATLAB programs. The examples of raw ultrasonic RF signal and results of it's processing are presented on Fig.2. As an example a raw ultrasound RF signal from 82-th line in B-scan is shown in top panel of Fig. 2 (a). The demodulated signal (IM) is presented in Fig. 2, (b). The software demodulated signal can be compared with the hardware demodulated signal given in bottom of original B-scan image (see Fig. 3, (a)). Strong echo pulse from the phantom target occurring at the depth of 22 mm is shown magnified on Fig.2, (c) and its amplitude spectra on Fig. 2, (d). We see significant downshift of echo central frequency from 7,5 MHz set in ultrasound system. This could be explained by influence of strong attenuation in Zerdine, which damps more higher frequencies than lower, and therefore downshift of central frequency is observed.

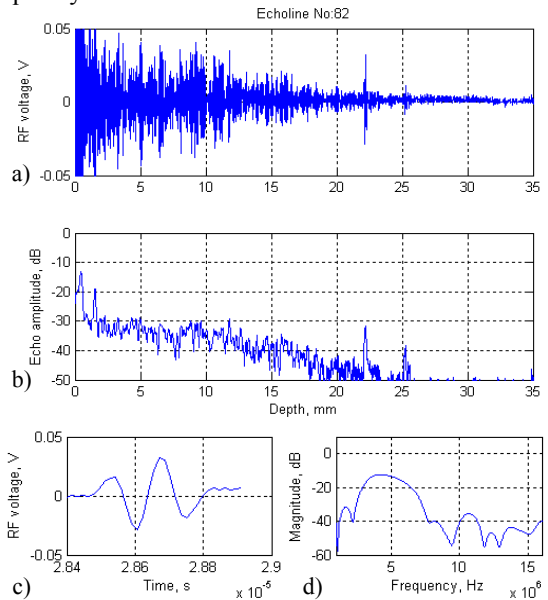


Fig. 2. B-scan data processing results: a – raw RF signal $x(t)$ from line Nr.82 of B-scan; b – calculated instantaneous magnitude $x_{IM}(t)$ of RF signal; c – pulse of echo from one-dimensional scatter; d – amplitude spectra of echo pulse

The conventional B-scan from the screen of Mentor Advent TM A/B scanner is presented in Fig. 3 (a). The instantaneous magnitude map synthesized on the screen of PC by the developed system is presented in Fig. 4. The IM parameter based B-scan map is presented using 0,08 normalized cut-off frequency 2nd order low pass filtering and logarithmic scale. Comparison with the original B-scan image on Fig. 3 shows the visual similarity of both images.

The parametric maps of frequency parameters of ultrasound RF signal were calculated according to (3, 4) equations and are presented in Figs. 5, 6. Mapping result on Fig. 5 shows the better homogeneity of the image and better lateral resolution when compared with amplitude mapping in Fig. 4.

Fig. 6 shows 2D maps from the central phantom region in depth 21-26 mm. The region on the map corresponds with neighboring reflections from two targets, therefore from the map one can estimate the point spread function (PSF). The isolines on the echo amplitude map are drawn at levels from -34 dB to -46 dB in -3 dB intervals.

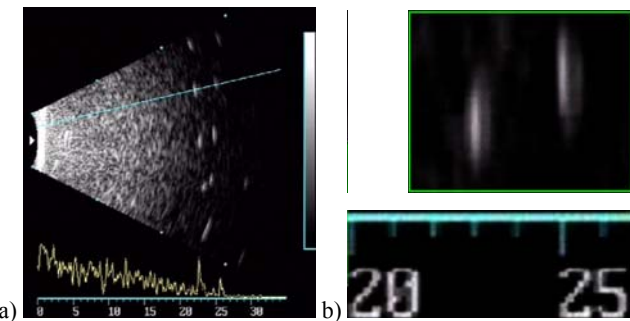


Fig. 3. The B scan acquired from reference points in CIRS Model 040 phantom (system acquisition parameters were: frequency 7,5 MHz, range 35 mm, gain 80 dB, velocity 1550 m/s, time gain control uniform for whole depth): a – original image; b – magnified image of points reflectors in center of B scan

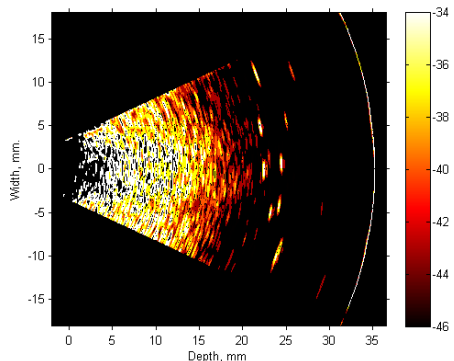


Fig. 4. Echo amplitude mapping result in case of phantom

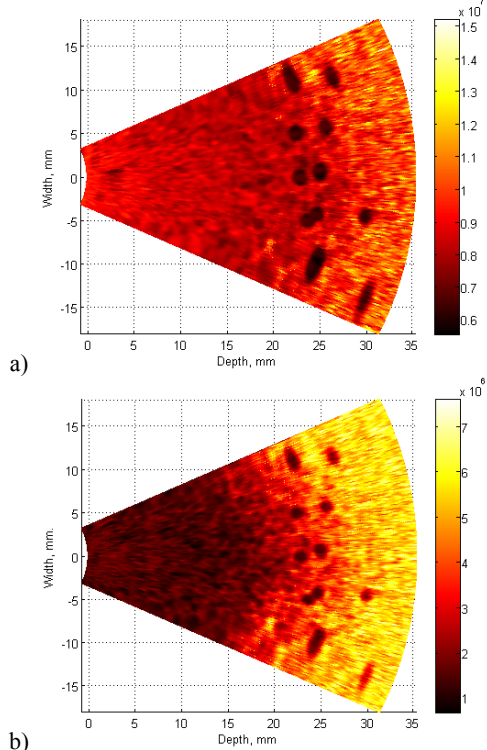


Fig. 5. Mapping spectral parameters of echo signal: a – mean instantaneous frequency; b – mean instantaneous bandwidth

MIB map shows isolines from 1 MHz to 3,5 MHz in intervals of 0,5 MHz. The details in amplitude and MIB maps show, that echo amplitude is the largest from start of one-dimensional target, but the MIB has minimum just after large echo amplitude. The displacement of MIB minimum from IM maximum is about 0,5 mm into the

depth. The true positions of targets are indicated with “+” signs in diagrams of Fig.6. The other interesting feature which was observed in frequency parameters maps is the different distributions of extreme values when comparing MIB and IM maps. In the MIB map small values dominate in the area of the map where strong backscattering from Zerdine microstructure takes place and also from point reflectors. From this point of view MIB map looks similar to IM map. The MIF map shows extreme values (minimums) only from point reflectors, eliminating backscattering from Zerdine microstructure. This differentiation could be used to facilitate differentiation of point reflectors in the strong background of backscattering.

The estimated dimensions of PSF are: axial - 0,2 mm and lateral - 1,9 mm in amplitude map at -6 dB level (peak amplitude was -30 dB). In case of MIB map we see that at the level of 1 MHz dimensions of PSF are: axial - 0,9 mm, lateral - 0,8 mm. (Amplitude spectra of echo pulse from plexiglass at 20 mm depth in water helped to estimate the bandwidth of ultrasonic transducer. The measured spectrum width is 8 MHz at the level of -30 dB.) It can be observed that mapping of frequency based parameter is able to improve lateral resolution up to two times at the price of decreasing the axial resolution which becomes worse up to four times. But here should be noted that frequency based mapping gives an image containing a new information potentially valuable for tissue characterization and differentiation.

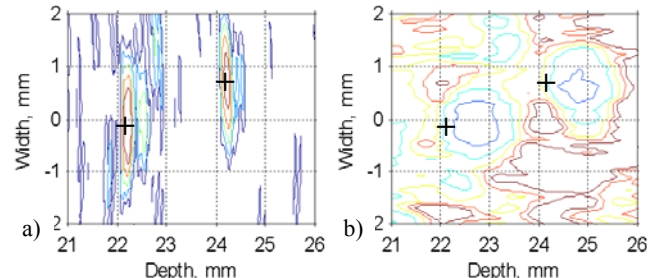


Fig. 6. Echo spread from one-dimensional targets in axial and lateral directions: a – mapping using IM; b – mapping using MIB

Conclusions

Ultrasonic B-scan radiofrequency signal acquisition and processing methodology was developed and a map of frequency-related parameters was synthesized. Evaluation of map resolution and comparison with conventional B-scan images obtained from reference targets in standard phantom have shown that parametric mapping gives a qualitatively new information about frequency dependent characteristics of the tissue and at the same time the resolution of the image remains comparable with conventional amplitude based mapping. The maps obtained using mean instantaneous frequency and bandwidth of radiofrequency echoscopy signal show different resolution features. We found that lateral resolution in B-scan image could be improved twice if mapping instantaneous bandwidth instead of instantaneous amplitude. The presented mapping technology could be easily modified for the development of new parametric maps by varying the parameter calculation algorithms. Parametric maps could be used for the differential diagnostics of the tissue.

Acknowledgment

This research was supported from Agency for International Science and Technology Development Programmes in Lithuania, EUROS TARS project E!4297 – NICDIT “A Non-Invasive Expert System for Diagnosis of Intraocular Tumours”.

References

1. Žakauskas M., Mačiulis A., Kopustinskas A., Paunksnis A., Kurapkienė S., Jegelevičius D. Echospectral Methods of Tissue Evaluation // Electronics and Electrical Engineering. – Kaunas: Technologija, 2004. – Nr. 7(56). – P. 70–73.
2. Paunksnis A., Kurapkienė S., Mačiulis A., Lukoševičius A., Špečkauskas M. The use of echospectral methods of tissue evaluation for follow-up of brachytherapy treatment // Ultrasound. – Kaunas: Technologija, 2007. – Nr. 4(62). – P. 45–48.
3. Coleman D. J., Silverman R. H., Rondeau M. J., Boldt H. C., Lloyd H. O., Lizzi F. L., Weingest T. A., Chen X., Vangveeravong S., Folberg R. Noninvasive in vivo detection of prognostic indicators for high-risk uveal melanoma: Ultrasound parameter imaging // Ophthalmology, 2004 March. – Vol. 111(3). – P. 558–564.
4. Torres V.L., Allemann N., Erwenne C.M., Ultrasound biomicroscopy features of iris and ciliary body melanomas before and after brachytherapy // Ophthalmic Surg Lasers Imaging, 2005 Mar–Apr. – Vol. 36(2). – P. 129–138.
5. John S., Sujana H., Suresh S., Swarnamani S., Biswas J., Gopal L. Ultrasonic characterisation of malignant melanoma of choroid // Indian J Ophthalmol, 1998 Sep. – Vol. 46(3). – P. 153–157.
6. Oelze M.L. Zachary J.F. Examination of cancer in mouse models using high-frequency quantitative ultrasound // Ultrasound in medicine & biology, 2006. – Vol. 32(11). – P. 1639–1648.
7. Paunksnis A., Barzdžiukas V., Kažys R.J., Raišutis R., Lukoševičius A., Paunksnis M., Janušauskas A., Marozas V., Jegelevičius D., Daukantas S., Kopsala S., Kurapkienė S., Kriauciūnienė L., Jurkonis R. A non-invasive expert system for diagnosis of intraocular tumours: the system concept // Ultrasound. – Kaunas: Technologija, 2008. – Nr. 4(63). – P. 66–72.
8. Auger F., Flandrin P., Lemoine O., Goncalves P. The Time–Frequency Toolbox, <<http://tftb.nongnu.org>>. Accessed 2008 Dec 7.
9. Домаркас В.Й., Пилецкас Э.Л. Ультразвуковая эхоскопия // Ленинград: Машиностроение, 1988. – 276 p.
10. General Purpose Multi-Tissue Ultrasound Phantom, Model 040, User Guide & Technical Information, Rev.06/17/08 // CIRS, Inc., Norfolk, Virginia, USA
11. Fujii Y., Taniguchi N., Itoh K., Shigeta K., Wang Y., Tsao J.-W., Kumasaki K., Itoh T., A New Method for Attenuation Coefficient Measurement in the Liver: Comparison With the Spectral Shift Central Frequency Method // J Ultrasound Med, 2002. – No. 21. – P. 783–788.

Received 2009 02 26

R. Jurkonis, S. Daukantas, A. Janušauskas, A. Lukoševičius, V. Marozas, D. Jegelevičius. Synthesis of Parametric Map from Raw Ultrasound B-Scan Data // Electronics and Electrical Engineering. – Kaunas: Technologija, 2009. – No. 6(94). – P. 109–112.

There are presented results of ultrasound radio-frequency signal sampling and processing to synthesize B-scan maps and evaluate two-dimensional visualization of ultrasound signal parameters. Our source of signal was ultrasound echoscope Mentor AdventTM A/B with mechanical scanning transducer of 11 MHz. Radio-frequency signal was digitized with digitizer Picoscope 5203. Amplitude and frequency based parameters were used for mapping B-scan ultrasound images. Standard phantom with axial resolution targets was used for the evaluation of mapping performance. We conclude that the signal processing and image transformation implemented in Matlab programs provide adequate two-dimensional mapping of B-scans. The usage of mean instantaneous bandwidth of radio frequency echoscopic signals enables to improve lateral resolution. Ill. 6, bibl. 11 (in English; summaries in English, Russian and Lithuanian).

Р. Юрконис, С. Даукантас, А. Янушаускас, А. Лукошевичюс, В. Марозас, Д. Ягялявичюс. Синтез параметрической карты из необработанных ультразвуковых данных Б-скана // Электроника и электротехника. – Каunas: Технология, 2009. – № 6(94). – С. 109–112.

В статье представлены результаты дискретизации и обработки ультразвуковых радиочастотных сигналов с целью синтезировать изображения Б-скана и исследовать двумерную визуализацию параметров ультразвуковых сигналов. Источником ультразвуковых сигналов был эхоскоп Mentor AdventTM A/B с преобразователем механического сканирования на 11 МГц. Сигналы оцифровывались с помощью устройства Picoscope 5203. Разрешающая способность исследовалась при помощи стандартного фантома. На изображении Б-скана были представлены не только амплитудные, но и частотные параметры эхосигналов. Работа позволяет сделать вывод, что программы обработки сигналов и трансформация изображения, реализованные в среде MATLAB, позволяют получить хорошие двухмерные карты Б-сканов. Применение параметров моментной частотной полосы спектра эхоскопических сигналов позволило улучшить поперечное разрешение. Ил. 6, библ. 11 (на английском языке; рефераты на английском, русском и литовском яз.).

R. Jurkonis, S. Daukantas, A. Janušauskas, A. Lukoševičius, V. Marozas, D. Jegelevičius. Parametrinių vaizdų sintezė naudojant neapdorotus ultragarsinius B skenavimo duomenis // Elektronika ir elektrotechnika. – Kaunas: Technologija, 2009. – Nr. 6(94). – P. 109–112.

Pateikiami ultragarsinių radijo dažninių signalų skaitmeninimo ir apdorojimo rezultatai siekiant sintezuoti B skenavimo vaizdus ir išvertinti dvimatių ultragarsinių signalų parametrų vaizdavimą. Signalų šaltinis buvo ultragarsinė echoskopinė sistema Mentor AdventTM A/B su 11 MHz mechaninio skenavimo keitikliu. Radijo dažninių signalas buvo skaitmenintas skaitmenikliu Picoscope 5203. Išvertintos dvimaičio vaizdavimo galimybės tiriant išilginio skiriamumo taikinius standartiniame fantome. B skenavimo vaizduose parodytos ne tik amplitudinės, bet ir dažninių echosignalų savybės. Šis tyrimas parodė, kad apdorojant signalus ir transformuojant vaizdus Matlab terpėje galima gauti adekvaciūs dvimaičius B skenavimo vaizdus. Naudojant radijo dažninių echoskopinio signalo vidutinį momentinį juostos plotį, galima pagerinti skersinį skiriamumą. Il. 6, bibl. 11 (anglų kalba; santraukos anglų, rusų ir lietuvių k.).